Derivation of Criterion Suitable for Evaluation of Multichannel Noise Reduction Systems for Speech Processing

Václav BOLOM, Jan INGERLE, Pavel SOVKA

Dept. of Circuit Theory, Czech Technical University in Prague, Technická 2, 166 27 Praha 6, Czech Rep.

bolomv1@fel.cvut.cz, jan@ingerle.cz, sovka@fel.cvut.cz

Abstract. *This paper deals with the theoretical derivation of the Noise Reduction criterion suitable for evaluation of multichannel noise reduction system performance. This criterion is suitable for noise suppression assessment and thus serves as an important step in the development of noise reduction systems. Noise reduction is evaluated in dependence on spatial coherence. The derivations are made for five basic multichannel systems, Delay and sum beamformer, Beamformer with adaptive postprocessing, Generalized sidelobe canceller, Linearly constrained beamformer, and Modified coherence filter.*

Keywords

Beamforming, microphone arrays, speech enhancement, noise reduction.

1. Introduction

Multichannel signal processing presents methods of spatial filtering. These methods are usually called beamforming. The algorithms use distribution of the signal sources in space. Multichannel or multi-microphone noise reduction systems are often used as preprocessors for speech processing and recognition. Multichannel methods are typically based on spatial filtering. These systems are usually called beamformers.

Beamforming applications are used in many fields, such as mobile communications, aids for hearing impaired persons, radioastronomy, seismology, etc. The results described in this paper are used for development of algorithms for speech enhancement. This application is suitable for hands-free communication in a car, or for teleconferencing.

This paper brings a theoretical derivation of the noise reduction (*NR*) criterion for five chosen basic algorithms of spatial filtering. The results will be used as a theoretical background for development of speech enhancement algorithms operating in a real environment.

Section 2 is an introduction to multichannel processing. It summarizes the basic information and assumptions. Section 3 presents three basic types of interferences in multichannel systems. Five chosen algorithms of spatial filtering are presented in Section 4. The *NR* criterion is defined in Section 5. A detailed analysis of chosen multichannel systems is performed in this section as well. An analytical derivation of the formulas for the *NR* calculation is the result of this section. The results of this section are then presented in Section 6, and they are also compared to simulations. A significance of the *NR* criterion for the evaluation and development of multichannel systems is discussed in Section 7.

2. Assumptions of the Evaluation of Multichannel Systems

Analyses have been made under the following assumptions. Omnidirectional and identical microphones are arranged into a uniform linear array (ULA) of M sensors with spacing D (see Fig. 1). Signal is sampled at each sensor. The source of the desired signal $s(t)$ is fixed and far enough from the array. So the wavefield appears as a plane wave at the array. The array is steered in the direction of arrival of the desired signal (the same samples of the desired signal appear at each sensor at the same time). Noise and interference are present at each sensor as well. Under these assumptions the k-th sample of the m-th sensor can be expressed as

$$x_m[k] = s[k] + u_m[k] \tag{1}$$

where $s[k]$ denotes the k-th sample of the desired signal, and $u_m[k]$ denotes noise and interference at the m-th sensor.

3. Interference in Multichannel Systems

Three types of interference are usually considered in a multichannel system. The types of interference are classified using their spatial properties, especially the coherence function. This function expresses the reciprocal dependency

(correlation) of particular signals in individual frequency bands. Coherence function $\Gamma_{ij}(e^{j\omega T})$ of two signals is defined by relation [15]

$$\Gamma_{ij}(e^{j\omega T}) = \frac{\phi_{ij}(e^{j\omega T})}{\sqrt{\phi_{ii}(e^{j\omega T})\phi_{jj}(e^{j\omega T})}} \tag{2}$$

where $\phi_{ii}(e^{j\omega T})$ denotes the power spectral density (PSD) of signal in the j-th channel, and $\phi_{ij}(e^{j\omega T})$ the cross-power spectral density (CPSD) of signals in the i-th and the j-th channel. The magnitude squared coherence (MSC) defined as

$$MSC(e^{j\omega T}) = \left|\Gamma_{ij}(e^{j\omega T})\right|^2 \tag{3}$$

is also often used.

The type of interference is distinguished according to the shape of the $MSC(e^{j\omega T})$. Three types of interferences are recognized: spatial coherent, spatial incoherent, and diffuse interference.

3.1 Spatial Coherent Interference

First, let us consider two spatial coherent signals. They are obtained in two different points of space (see Fig. 1) and are correlated in the whole frequency band. To verify this statement, let us consider the plane wavefront reaching sensors 1 and 2 under angle φ_c (Fig. 1). The spectrum of signal at sensor 2 is $X_2(e^{j\omega T})$. The wavefront reaching sensor 1 is attenuated by a constant A and delayed by

$$\tau = \frac{D}{c}\cos\varphi_c \tag{4}$$

where c denotes the propagation speed of an acoustic signal. The spectrum of signal at sensor 1 is given by

$$X_1(e^{j\omega T}) = A\, X_2(e^{j\omega T})e^{-j\omega\tau}. \tag{5}$$

Substituting (5) into (2) results into an expression for the coherence function:

$$\Gamma_{12}(e^{j\omega T}) = \frac{A\,\phi_{22}(e^{j\omega T})e^{-j\omega\tau}}{\sqrt{A^2\phi_{22}(e^{j\omega T})\phi_{22}(e^{j\omega T})}} = \\ = e^{-j\omega\frac{D}{c}\cos\varphi_c}. \tag{6}$$

Thus the expression for $MSC(e^{j\omega T})$ reveals full coherency

$$MSC(e^{j\omega T}) = \left|\Gamma_{12}(e^{j\omega T})\right|^2 = 1. \tag{7}$$

Spatial coherent noise is typically created by car engine and fan.

3.2 Spatial Incoherent Interference

In case of spatial incoherent interference, the coherence computed from samples obtained at two different points in space is equal to zero in the whole frequency band because $E[X_1^*(e^{j\omega T})X_2(e^{j\omega T})] = 0$. X_1 and X_2 denote the spectra of two interferences and the asterisk denotes complex conjugate.

Spatial incoherent noise is generated by microphones and by electrical equipment.

3.3 Spatial Diffuse Interference

A spatial diffuse signal is a specific type of signal which originates in a limited number of sources in a reverberant environment. The delayed signal reaches the array together with the direct wave. The presence of the delayed signal is caused by reflections. The characteristics of the delayed signal (magnitude and phase) depend on the acoustic properties of the given environment, e.g. room. This type of interference is very often present in a real environment.

In literature dealing with diffuse noise in multichannel speech enhancing systems [3] a model of noise is assigned. The model consists of independent sources of interference placed on a sphere. A formula for coherence derived from this model is given by

$$\Gamma_{12}(e^{j\omega T}) = \frac{\sin(\frac{\omega D}{c})}{\frac{\omega D}{c}} \tag{8}$$

where ω denotes angular frequency while D and c have been defined above. A shape of diffuse noise is depicted in Fig. 2. The shapes are depicted for microphone spacing $D = 5$ cm, 10 cm, and 20 cm. Analysis of the equation (8) and Fig. 2 shows that the closer together the microphones are placed, the wider the main lobe of MSC is.

Diffuse noise is generated in enclosed rooms by reverberation.

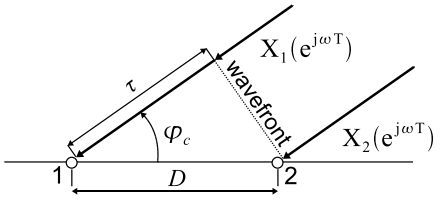

Fig. 1. An array of two sensors.

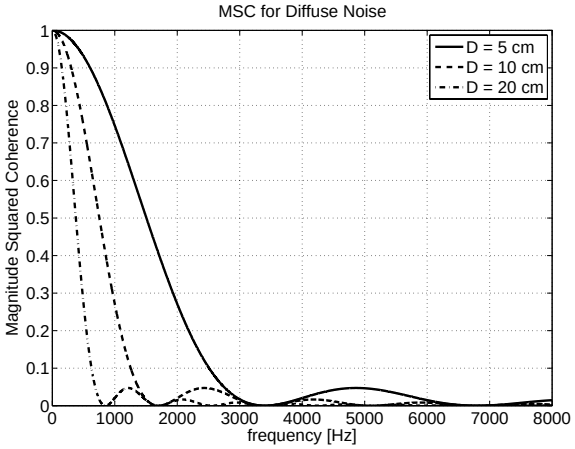

Fig. 2. The MSC for diffuse noise and different microphone spacing.

4. Chosen Algorithms of Array Processing

Multichannel noise reduction systems are typically composed of three main parts, the Delay and sum beamformer (DAS), Wiener filter (WF), and Adaptive noise canceller (ANC). The DAS beamformer uses spatial information to reduce additive noise contaminating speech in noisy environment. The ANC and WF use some type of filtration to further suppress incoherent and coherent noise, respectively. These parts can be combined to give five following systems.

The first one, the Delay and sum beamformer, is a basic unit for the following beamformers: Beamformer with adaptive postprocessing (BAP), Generalized sidelobe canceler (GSC), Linearly constrained beamformer (LCB), and Modified coherence filtering (MCF).

4.1 DAS

The structure of the DAS beamformer is depicted in Fig. 3 (labels in all figures are supposed to be spectra of signals). The input samples are multiplied by weights $w_i = \frac{1}{M}$, $i = 1,...,M$ and summed. The advantage of this beamformer is its simplicity [16], [7] and independence of weights on the signal characteristics. Its disadvantage is a low enhancement of the desired signal.

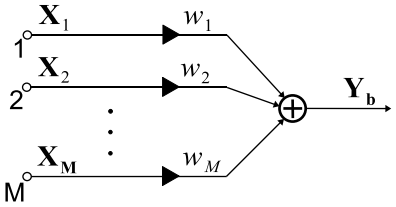

Fig. 3. DAS.

4.2 BAP

Beamformer with adaptive postprocessing [19] improves the DAS beamformer by using a Wiener filter (WF) behind the DAS structure, Fig. 4. The main contribution of WF is improving the suppression level of uncorrelated interferences. The derivation for the weights of WF can be found in [18]. Weights in the frequency domain are obtained as

$$W(e^{j\omega T}) = \frac{\phi_{xs}(e^{j\omega T})}{\phi_{xx}(e^{j\omega T})} \tag{9}$$

where $\phi_{xx}(e^{j\omega T})$ denotes the power spectral density (PSD) of signal $x[k]$ (input of WF), and $\phi_{xs}(e^{j\omega T})$ is the cross-power spectral density (CPSD) of signals $x[k]$ and $s[k]$ (output of WF). It is assumed that the interferences are uncorrelated ($E[U_i(e^{j\omega T})U_j(e^{j\omega T})] = 0$ for all $i \neq j$) and that the desired signal is uncorrelated with interferences ($E[S(e^{j\omega T})U_i(e^{j\omega T})] = 0$ for all i). $S(e^{j\omega T})$ is a spectrum of the desired signal and $U_i(e^{j\omega T})$ is a spectrum of the interference at the i-th sensor. Under these assumptions it holds

$$\phi_{xs}(e^{j\omega T}) = \phi_{sx}(e^{j\omega T}) = \phi_{ss}(e^{j\omega T}). \tag{10}$$

Weights of WF can now be expressed as

$$W(e^{j\omega T}) = \frac{\phi_{ss}(e^{j\omega T})}{\phi_{xx}(e^{j\omega T})}. \tag{11}$$

In the case of the BAP structure, the PSDs in relation (11) are estimated by averaging the signal in a particular channel [13]

$$\hat{\phi}_{ss} = \frac{2}{M(M-1)} \sum_{i=1}^{M-1} \sum_{k=i+1}^{M} Re\left\{X_i(e^{j\omega T})^* X_k(e^{j\omega T})\right\} \tag{12}$$

$$\hat{\phi}_{xx}(e^{j\omega T}) = \left| \frac{1}{M} \sum_{i=1}^{M} X_i(e^{j\omega T}) \right|^2 \tag{13}$$

where $X_i(e^{j\omega T})$ is a spectrum of the input signal.

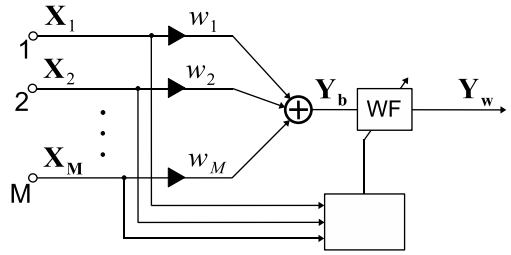

Fig. 4. BAP.

4.3 GSC

The structure of GSC [6] is depicted in Fig. 5. It is equal to the adaptive beamformer [5]. The system consists of the DAS beamformer and the adaptive noise canceler (ANC). ANC serves to suppress the coherent interference.

The weights of the ANC filters are computed according to Wiener theory [6]. A formula for optimal weights is given by

$$H_i(e^{j\omega T}) = \frac{\phi_{Y_i Y_b}(e^{j\omega T})}{\phi_{Y_i Y_i}(e^{j\omega T})}, \qquad i = 1,\ldots,M-1. \tag{14}$$

$\phi_{Y_i Y_b}$ denotes the CPSD of signals Y_i and Y_w (see Fig. 5). $\phi_{Y_i Y_i}$ is the PSD of Y_i.

The proper function of the ANC is given by perfect separation of the desired signal from the input signal. Let us denote any coherent signal incident on the array from any direction except the DOA as coherent interference. Under this assumption, an interference can be separated from the input signal by an appropriate combination of input channels $x_i[k]$. This separation is arranged by the blocking matrix (BM). The most commonly used BM differentiates neighboring channels. BM consists of M columns and $(M-1)$ rows, and looks like this [6]:

$$BM = \begin{pmatrix} 1 & -1 & 0 & \ldots & 0 & 0 \\ 0 & 1 & -1 & \ldots & 0 & 0 \\ \vdots & \vdots & \vdots & \ddots & \vdots & \vdots \\ 0 & 0 & 0 & \ldots & 1 & -1 \end{pmatrix}. \tag{15}$$

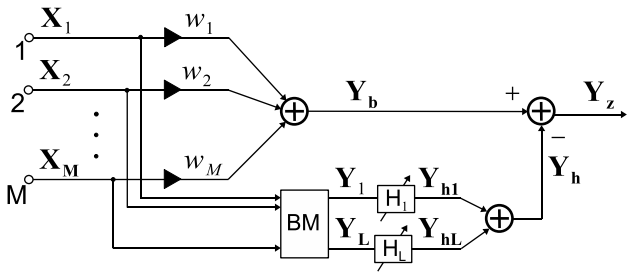

Fig. 5. GSC.

4.4 LCB

LCB utilizes GSC and BAP beamformers [4]. The structure of LCB is depicted in Fig. 6.

The direct branch composed of BAP suppresses incoherent interference. The lower branch consisting of ANC is responsible for coherent interference suppression.

The greatest difference between GSC and LCB is the way in which the weights of ANC filters are computed. In LCB, they are computed from signals at the outputs of BM and WF. The relation for calculating the ANC filters has to be written as

$$H_i(e^{j\omega T}) = \frac{\phi_{Y_i Y_w}(e^{j\omega T})}{\phi_{Y_i Y_i}(e^{j\omega T})}, \qquad i = 1,\ldots,M-1. \tag{16}$$

$\phi_{Y_i Y_w}$ denotes the CPSD of signals Y_i and Y_w the meaning of which is obvious from Fig. 6.

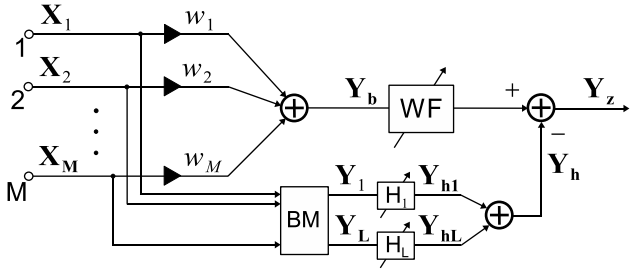

Fig. 6. LCB.

4.5 Coherence Filtering

Coherence filtering is a representative of double channel methods. The idea of this method [2] is based on the fact that the coherence function of the spatially coherent desired signal is close to one, and the coherence of the incoherent interference is close to zero.

The algorithm is usually implemented in the frequency domain. The number of frequency bands is given by the dimension of the Fourier transform. First, the coherence function between two channels is computed according to the equation (2). Further processing is given by the value of the coherence function at individual spectral band k.

Two thresholds S_{max} and S_{min} are introduced for determination of coefficients of the coherence filter. The coefficients $C_{CF}(k)$ are computed as follows

$$C_{CF}(k) = \begin{cases} 1, & \text{if } \Gamma^2(k) > S_{max}, \\ (\Gamma^2(k))^{\alpha}, & \text{if } S_{min} \le \Gamma^2(k) \le S_{max} \\ |S_{min}|^{\alpha}, & \text{if } \Gamma^2(k) < S_{min} \end{cases} \tag{17}$$

where α represents an integer exponent.

The authors of the [8] propose a modification to coherence filtering. The coherence filter is included in the BAP structure (see Fig. 7). The number of thresholds is reduced from two to one. The coefficients of the Modified coherence filter (MCF) $C(k)$ are computed as follows

$$C(k) = \begin{cases} W(k), & \text{if } |\Gamma(k)| > T \\ |\Gamma(k)|^{\alpha}, & \text{if } |\Gamma(k)| \le T \end{cases} \tag{18}$$

where $W(k)$ denotes an estimated frequency response of the Wiener filter (9), and T denotes the threshold.

There is another approach how to compute coherence. It can be computed between an arbitrary input channel X_i and the output of DAS Y_b. This modification will be called MCF2.

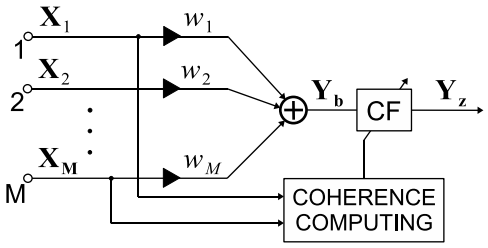

Fig. 7. Structure of Modified coherence filter.

5. Beamformer Evaluation

For the evaluation of beamformers in presence of interference, several criteria can be used, e.g. directivity pattern, directivity index, noise reduction, etc. Directivity properties have been discussed in [17]. This paper is focused on the evaluation of the described beamformers using NR.

5.1 Noise Reduction

The Noise reduction (NR) is defined as [9]

$$NR(e^{j\omega T}) = 10\log \left. \frac{\phi_{uu}(e^{j\omega T})}{\phi_{y_u y_u}(e^{j\omega T})} \right|_{\phi_{ss}=0} \tag{19}$$

where $\phi_{uu}(e^{j\omega T})$ denotes the PSD of interference at the input of the system, and $\phi_{y_u y_u}(e^{j\omega T})$ the PSD of interference at the output of the system. The NR can be easily analytically expressed in dependence on coherence. The NR shows dependence of the algorithm on the type of noise. Note that this criterion does not show the influence of the beamformer on the desired signal. It is assumed that no desired signal is present at the input of the system during computing of the NR.

5.2 NR Evaluation of Beamformers

All variables in further derivations are supposed to be

in the frequency domain (the parenthesis $(e^{j\omega T})$ will be omitted for better readability).

For the *NR* derivation the input signal is assumed to be a homogenous acoustic wavefield. Under these assumptions it holds

$$\begin{aligned} \phi_{u_i u_i} &= \phi_{uu}, \\ \phi_{s_i s_i} &= \phi_{ss}. \end{aligned} \tag{20}$$

The desired signal and the interference are supposed to be proportionally independent:

$$E[X_u X_s] = 0. \tag{21}$$

This assumption implies a relation for the PSDs:

$$\phi_{X_i X_j} = \phi_{s_i s_j} + \phi_{u_i u_j}. \tag{22}$$

In the following derivations the average coherence function will be used

$$\bar{\Gamma} = \frac{2}{M^2 - M} \sum_{i=1}^{M-1} \sum_{j=i+1}^{M} Re\{\Gamma_{ij}\}. \tag{23}$$

5.3 DAS

Utilizing the presumptions mentioned above, for the PSD of the DAS output Y_b it holds [10]:

$$\begin{aligned} \phi_{Y_b Y_b} &= E[Y_b Y_b^*] = E\left[\left(\frac{1}{M}\sum_{i=1}^{M} X_i\right)\left(\frac{1}{M}\sum_{i=1}^{M} X_i^*\right)\right] = \\ &= \frac{1}{M^2}\sum_{i=1}^{M}\sum_{j=1}^{M} E[X_i X_j^*] = \frac{1}{M^2}\sum_{i=1}^{M}\sum_{j=1}^{M}\phi_{X_i X_j} = \\ &= \frac{1}{M^2}\sum_{i=1}^{M}\phi_{X_i X_i} + \frac{2}{M^2}\sum_{i=1}^{M-1}\sum_{j=i+1}^{M} Re\left\{\phi_{X_i X_j}\right\} = \\ &= \left|\phi_{ss} = 0\right| = \\ &= \frac{1}{M^2}\sum_{i=1}^{M}(\phi_{u_i u_i}) + \frac{2}{M^2}\sum_{i=1}^{M-1}\sum_{j=i+1}^{M} Re\left\{\phi_{u_i u_j}\right\} = \\ &= \frac{1}{M}\phi_{uu} + \frac{2}{M^2}\phi_{uu}\sum_{i=1}^{M-1}\sum_{j=i+1}^{M} Re\left\{\Gamma_{u_i u_j}\right\} = \\ &= \left[\frac{1}{M} + \left(1 - \frac{1}{M}\right)\bar{\Gamma}_{uu}\right]\phi_{uu}. \end{aligned} \tag{24}$$

Final NR_{DAS} expression is then given by

$$NR_{DAS} = \left.\frac{\phi_{uu}}{\phi_{Y_b Y_b}}\right|_{\phi_{ss}=0} = \frac{1}{\frac{1}{M} + \left(1 - \frac{1}{M}\right)\bar{\Gamma}_{uu}}. \tag{25}$$

5.4 BAP

The PSD of the output signal of BAP is expressed by formula

$$\phi_{Y_w Y_w} = W^2 \phi_{Y_b Y_b}. \tag{26}$$

The meaning of all variables is obvious from Fig. 4.

Substituting (13), (12), and (10) into (9), an expression for weights of WF is obtained:

$$W = \frac{\frac{2}{M(M-1)}\sum_{i=1}^{M-1}\sum_{j=i+1}^{M} Re\{X_i^* X_j\}}{\left|\frac{1}{M}\sum_{i=1}^{M} X_i\right|^2}. \tag{27}$$

The transfer function of WF can be written as a function of the coherence. The denominator of this function has already been expressed by (24). The nominator is expressed as follows

$$\begin{aligned} \hat{\phi}_{ss} &= \frac{2}{M(M-1)}\sum_{i=1}^{M-1}\sum_{j=i+1}^{M} Re\left\{\phi_{x_i x_j}\right\} = \\ &= \left|\phi_{s_i s_j} = 0\right| = \\ &= \frac{2}{M(M-1)}\sum_{i=1}^{M-1}\sum_{j=i+1}^{M} Re\left\{\phi_{u_i u_j}\right\} = \\ &= \frac{2}{M(M-1)}\sum_{i=1}^{M-1}\sum_{j=i+1}^{M} Re\left\{\phi_{uu}\,\Gamma_{u_i u_j}\right\} = \\ &= \phi_{uu}\bar{\Gamma}_{uu}. \end{aligned} \tag{28}$$

The relation (27) can be rewritten as a function of the average coherence in the form

$$W = \frac{\bar{\Gamma}_{uu}}{\frac{1}{M} + \left(1 - \frac{1}{M}\right)\bar{\Gamma}_{uu}}. \tag{29}$$

Utilizing this expression and (26), NR_{BAP} can be expressed as

$$NR_{BAP} = \left.\frac{\phi_{uu}}{W^2 \phi_{Y_b Y_b}}\right|_{\phi_{ss}=0} = \frac{\frac{1}{M} + \left(1 - \frac{1}{M}\right)\bar{\Gamma}_{uu}}{\bar{\Gamma}_{uu}^2}. \tag{30}$$

5.5 GSC

The complete derivation of *NR* formula for GSC will be given now. The structure of GSC is depicted in Fig. 5. Under condition of $\phi_{ss} = 0$ it holds $Y_h = Y_b$. The ANC branch performs estimation of the interference. Using relations (2), (20), and (21) CPSD of signals Y_i, and Y_b is expressed as

$$\begin{aligned}\phi_{Y_iY_b} &= (X_i - X_{i+1})\frac{1}{M}\sum_{k=1}^{M} X_k^* = \\ &= \frac{1}{M}\left(\sum_{k=1}^{k<i} X_iX_k^* + |X_i|^2 + \sum_{k=i+1}^{M} X_iX_k^* - \right. \\ &\left. - \sum_{k=1}^{k\le i} X_{i+1}X_k^* - |X_{i+1}|^2 - \sum_{k=i+2}^{M} X_{i+1}X_k^*\right) = \\ &= \frac{1}{M}\left(\sqrt{\phi_{X_iX_i}\phi_{X_kX_k}}\sum_{k=1}^{k<i}\Gamma_{X_iX_k} + \right. \\ &+ \sqrt{\phi_{X_iX_i}\phi_{X_kX_k}}\sum_{k=i+1}^{M}\Gamma_{X_iX_k} - \\ &- \sqrt{\phi_{X_{i+1}X_{i+1}}\phi_{X_kX_k}}\sum_{k=1}^{j\le i}\Gamma_{X_{i+1}X_k} - \\ &\left. - \sqrt{\phi_{X_{i+1}X_{i+1}}\phi_{X_kX_k}}\sum_{j=i+2}^{M}\Gamma_{X_{i+1}X_k}\right) = \left|\phi_{s_is_j} = 0\right| = \\ &= \frac{\phi_{uu}}{M}\left(\sum_{k=1}^{k<i}\Gamma^{u*}_{X_kX_i} + \sum_{k=i+1}^{M}\Gamma^{u}_{X_iX_k} - \right. \\ &\left. - \sum_{k=1}^{k\le i}\Gamma^{u*}_{X_kX_{i+1}} - \sum_{k=i+2}^{M-1}\Gamma^{u}_{X_{i+1}X_k}\right) = \frac{\phi_{uu}}{M}(\mathfrak{A})\end{aligned} \tag{31}$$

where $\Gamma^u_{X_iX_k}$ denotes the coherence between the channels i and k under the assumption that no desired signal is present at the input of the system. Symbol $\mathfrak{A}$ is used for better readability of the further text. The PSD of Y_i can be written subject to the same condition:

$$\begin{aligned}\phi_{Y_iY_i} &= E[(X_i - X_{i+1})(X_i - X_{i+1})^*] = \\ &= E[|X_i|^2] + E[|X_{i+1}|^2] - 2E[Re\{X_iX_{i+1}^*\}] = \\ &= \phi_{X_iX_i} + \phi_{X_{i+1}X_{i+1}} - \\ &- 2\sqrt{\phi_{X_iX_i}\phi_{X_{i+1}X_{i+1}}}Re\{\Gamma_{X_iX_{i+1}}\} = \left|\phi_{s_is_j} = 0\right| = \\ &= 2\phi_{uu}\left(1 - Re\left\{\Gamma^u_{X_iX_{i+1}}\right\}\right).\end{aligned} \tag{32}$$

For better orientation in formulas, symbol $\heartsuit$ is set. The meaning of this symbol is reciprocal of NR_{DAS} (25).

$$\heartsuit = \frac{1}{M} + \left(1 - \frac{1}{M}\right)\bar{\Gamma}_{uu}. \tag{33}$$

Under condition $\phi_{ss} = 0$, the output of GSC is $Y_z = Y_b - Y_h$. The samples of Y_z should be equal to zero. Interference present in Y_b is estimated by ANC filter. Subject to the assumption that the weights of the ANC are optimal, Y_h is equal to Y_b. The NR for the structure behind DAS in GSC can be expressed as

$$\begin{aligned}NR_{post} &= \left.\frac{\phi_{Y_bY_b}}{\phi_{Y_zY_z}}\right|_{\phi_{ss}=0} = \left.\frac{\phi_{Y_bY_b}}{\phi_{Y_bY_b} - \phi_{Y_hY_h}}\right|_{\phi_{ss}=0} = \\ &= \left.\frac{\phi_{Y_bY_b}}{\phi_{Y_bY_b} - \frac{1}{M-1}\sum_{i=1}^{M-1}|H_i|^2\phi_{Y_iY_i}}\right|_{\phi_{ss}=0} = \\ &= \left|H_{opt} = \frac{\phi_{Y_iY_b}}{\phi_{Y_iY_i}}\right| = \\ &= \left.\frac{1}{1 - \frac{1}{(M-1)\phi_{Y_bY_b}}\sum_{i=1}^{M-1}\left|\frac{\phi_{Y_iY_b}}{\phi_{Y_iY_i}}\right|^2\phi_{Y_iY_i}}\right|_{\phi_{ss}=0} = \\ &= \frac{1}{1 - \frac{1}{M-1}\sum_{i=1}^{M-1}\frac{|\mathfrak{A}|^2}{2M^2\left(1 - Re\left\{\Gamma^u_{X_iX_{i+1}}\right\}\right)\heartsuit}}.\end{aligned} \tag{34}$$

This formula agrees with the results given in [1], where the idea to evaluate GSC using the NR was suggested.

NR of GSC can be now written as

$$\begin{aligned}NR_{GSC} &= \left.\frac{\phi_{uu}}{\phi_{Y_zY_z}}\right|_{\phi_{ss}=0} = \left.\frac{\phi_{Y_bY_b}}{\phi_{Y_zY_z}}\frac{\phi_{uu}}{\phi_{Y_bY_b}}\right|_{\phi_{ss}=0} = \\ &= NR_{post}\left.\frac{\phi_{uu}}{\phi_{bb}}\right|_{\phi_{ss}=0} = \\ &= \frac{1}{\heartsuit - \frac{1}{2M^2(M-1)}\sum_{i=1}^{M-1}\frac{|\mathfrak{A}|^2}{1 - Re\left\{\Gamma^u_{X_iX_{i+1}}\right\}}}.\end{aligned} \tag{35}$$

5.6 LCB

LCB is a combination of BAP and GSC. The PSD of the output $\phi_{Y_zY_z}$ is given by combination of the output PSDs of these beamformers:

$$\begin{aligned}\phi_{Y_zY_z} &= \phi_{Y_wY_w} - \phi_{Y_hY_h} = \\ &= |W|^2\phi_{Y_bY_b} - \frac{1}{M-1}\sum_{i=1}^{M-1}|H_i|^2\phi_{Y_iY_i} = \\ &= \left|W_{opt} = \frac{\phi_{\hat{s}\hat{s}}}{\phi_{Y_bY_b}}; H_{opt} = \frac{\phi_{Y_iY_w}}{\phi_{Y_iY_i}} = \frac{Y_i^*Y_w}{\phi_{Y_iY_i}} = \right. \\ &\left. = \frac{Y_i^*W_{opt}Y_b}{\phi_{Y_iY_i}} = W_{opt}\frac{\phi_{Y_iY_b}}{\phi_{Y_iY_i}}\right| = \\ &= \left|\frac{\phi_{\hat{s}\hat{s}}}{\phi_{Y_bY_b}}\right|^2\left(1 - \frac{1}{M-1}\sum_{i=1}^{M-1}\frac{\left|\phi_{Y_iY_b}\right|^2}{\phi_{Y_iY_i}\phi_{Y_bY_b}}\right).\end{aligned} \tag{36}$$

For better readability, the calculation of the NR_{LCB} is divided into two steps. The NR_{post} of LCB upper branch behind the DAS beamformer is given by

$$NR_{post} = \left.\frac{\phi_{Y_bY_b}}{\phi_{Y_zY_z}}\right|_{\phi_{ss}=0} = \\ = \frac{1}{\left|\frac{\phi_{\hat{s}\hat{s}}}{\phi_{Y_bY_b}}\right|^2\left(1-\frac{1}{M-1}\sum_{i=1}^{M-1}\frac{|\phi_{Y_iY_b}|^2}{\phi_{Y_iY_i}\phi_{Y_bY_b}}\right)} = \\ = \frac{1}{\frac{\bar{\Gamma}_{uu}^2}{\heartsuit^2}\left(1-\frac{1}{2M^2(M-1)}\sum_{i=1}^{M-1}\frac{|\mathfrak{A}|^2}{\left(1-Re\left\{\Gamma^u_{X_iX_{i+1}}\right\}\right)\heartsuit}\right)}. \tag{37}$$

The final formula for the NR_{LCB} is obtained as

$$NR_{LCB} = NR_{post}\left.\frac{\phi_{uu}}{\phi_{Y_bY_b}}\right|_{\phi_{ss}=0} = \\ = \frac{1}{\frac{\bar{\Gamma}_{uu}^2}{\heartsuit}\left(1-\frac{1}{2M^2(M-1)}\sum_{i=1}^{M-1}\frac{|\mathfrak{A}|^2}{\left(1-Re\left\{\Gamma^u_{X_iX_{i+1}}\right\}\right)\heartsuit}\right)}. \tag{38}$$

5.7 Modified Coherence Filtering

The coefficients of the Coherence filter are given by (18). Behavior of the filter for $\mathrm{T} > \Gamma(k)$ is the same as BAP beamformer (30). Thus, only a case of $\mathrm{T} \leq \Gamma(k)$ will be investigated.

The *NR* of the Modified coherence filter (MCF) for $\mathrm{T} \leq \Gamma(k)$ can be expressed as

$$NR_{MCF} = \left.\frac{\phi_{uu}}{\phi_{Y_zY_z}}\right|_{\phi_{ss}=0} = \frac{\phi_{uu}}{\phi_{Y_bY_b}}\cdot\left.\frac{\phi_{Y_bY_b}}{\phi_{Y_zY_z}}\right|_{\phi_{ss}=0} = \\ = NR_{DAS}NR_{post}. \tag{39}$$

In the first case the NR_{post} will be derived for Γ_{ij} computed between two arbitrary channels i and j. The equation (24) for Φ_{YbYb} and relation (18) for MCF will be utilized.

$$NR_{MCF} = NR_{post\,\Gamma<\mathrm{T}}\left.\frac{\phi_{uu}}{\phi_{Y_zY_z}}\right|_{\phi_{ss}=0} = \left.\frac{\phi_{uu}}{C^2\phi_{Y_bY_b}}\right|_{\phi_{ss}=0} = \\ = \frac{\phi_{uu}}{C^2\phi_{uu}\left(\frac{1}{M}+\left(1-\frac{1}{M}\right)\bar{\Gamma}_{uu}\right)} = \\ = \frac{1}{|\Gamma_{ij}|^{2\alpha}\left(\frac{1}{M}+\left(1-\frac{1}{M}\right)\bar{\Gamma}_{uu}\right)}. \tag{40}$$

In case that the coherence is computed between one input channel i and the output of the DAS beamformer Y_b (MCF2), the situation is a little more difficult. It is necessary to derive the relation for the coherence $\Gamma_{X_iY_b}$.

$$\phi_{X_iY_b} = E[X_iY_b^*] = \frac{1}{M}\sum_{j=1}^{M}E[X_iX_J^*] = \\ = \frac{1}{M}\sum_{j=1}^{M}\phi_{X_iX_j} = \frac{\phi_{uu}}{M}\sum_{j=1}^{M}\Gamma_{ij}. \tag{41}$$

NR_{post} for this MCF2 can be now derived.

$$NR_{post} = \left.\frac{\phi_{Y_bY_b}}{\phi_{Y_zY_z}}\right|_{\phi_{ss}=0} = \left.\frac{\phi_{Y_bY_b}}{C^2\phi_{Y_bY_b}}\right|_{\phi_{ss}=0} = \frac{1}{C^2} = \\ = \frac{1}{|\Gamma_{X_iY_b}|^{2\alpha}} = \frac{1}{\left|\frac{\phi_{X_iY_b}}{\sqrt{\phi_{X_iX_i}\phi_{Y_bY_b}}}\right|^{2\alpha}} = \\ = \left(\frac{\phi_{X_iX_i}\left(\frac{1}{M}+\left(1-\frac{1}{M}\right)\bar{\Gamma}_{uu}\right)\phi_{uu}}{|\phi_{X_iY_b}|^2}\right)^{\alpha} = \\ = \left(\frac{\frac{1}{M}+\left(1-\frac{1}{M}\right)\bar{\Gamma}_{uu}}{|\frac{1}{M}\sum_{j=1}^{M}\Gamma_{X_iX_j}|^2}\right)^{\alpha}. \tag{42}$$

The whole expression for the *NR* of the whole MCF2 NR_{CF} can be derived according to (39)

$$NR_{MCF2} = \frac{\left(\frac{1}{M}+\left(1-\frac{1}{M}\right)\bar{\Gamma}_{uu}\right)^{\alpha-1}}{|\frac{1}{M}\sum_{j=1}^{M}\Gamma_{X_iX_j}|^{2\alpha}}. \tag{43}$$

6. Results of Analyses and Simulations

Analyses of the formulas derived in Section 5.2 will be presented in this section. Theoretical shapes of the *NR* for five systems will be compared to the results of simulations as well. Each system is analyzed for coherent and diffuse noise separately. Finally, all the systems will be compared.

6.1 Analysis Conditions

Theoretical shapes of the *NR* (analyses) are obtained by inserting the coherence $\Gamma_{uu}(e^{\mathrm{j}\omega T})$ in an expression for the *NR*. In the case of coherent noise, the coherence $\Gamma_{uu}(e^{\mathrm{j}\omega T})$ is given by generalization of (6). The direction of arrival of interference is set to $\phi_c = 60^\circ$. The coherence of diffuse noise is obtained by generalization of (8).

The analyses are performed for a number of microphones $M = 2, 4, 8$. Microphone spacing is set to 5 cm and sound velocity to $c = 340$ m/s. The systems are analyzed in the frequency range $0 - 8$ kHz.

6.2 Simulation Conditions

The theoretical results derived in Section 5 are compared to the results of simulations. The simulation are performed for both coherent and diffuse noise. The conditions of the simulations are chosen to match the conditions of the analyses. The testing signals are generated for a uniformly spaced linear array of four microphones with microphone spacing $D = 5$ cm. Sampling frequency is set to 16 kHz so that the result covers the frequency band 0 – 8 kHz.

Coherent noise is generated in the following way. The first channel is represented by the Gaussian noise. This sig-

nal is delayed in the second to fourth channel. The delay in each channel corresponds to the arrival of the plane wave impinging the array under the angle $\phi_c = 60^\circ$. The delay in each channel is expressed by relation $\tau = \frac{d}{c}\cos\phi_c$, where d denotes the distance of the microphone from the first microphone. It is necessary to delay the signal by the non-integer value. This operation is performed by a modification of the phase spectrum [14]. A comparison of the MSC between the first and the second channel for a model and for a simulation is depicted in Fig. 8. In the case of the simulation, the MSC is a little less than 1 in the whole frequency band.

A model of diffuse noise described in [11] and mentioned in Section 3 is used for generation of diffuse noise. 1124 sources of the Gaussian noise are uniformly placed on a sphere with its center in the center of the array. The signal at the i-th microphone is obtained as a sum of contributions from each source. A comparison of the MSC between the first and the second channel for a model and for a simulation is depicted in Fig. 9.

The systems are evaluated in the following way. The input signal described above is put at the input of the system. Then, the signal is processed by the system. The PSD of the input and output signal is then estimated via Welch's method. The length of the window is 16 ms with 50 % overlap. The total length of the testing signal is 1 s. The estimated PSD is finally used for calculation of the NR according to (19).

6.3 DAS

The shapes of the NR for DAS are depicted in Figs. 10 to 13. Fig. 10 depicts the NR_{DAS} for coherent noise. The shapes for 2, 4 and 8 microphones are compared in this graph. The shapes show peaks at some frequencies. It is caused by zero values of denominator of the formula 25 for NR_{DAS}. The position of these peaks can be easily found in the case of an array of two microphones. By inserting the average coherence 23 for coherent interference 6, the denominator of the NR_{DAS} $\frac{1}{M} + \left(1 - \frac{1}{M}\right)\cos\left(\omega\frac{D}{c}\cos\phi_c\right)$ is obtained. This relation is equal to zero in the case of $M = 2$ for $f = \frac{c}{2D\cos\phi_c} + k \cdot \frac{c}{D\cos\phi_c}$, where k is integer. Position of this peak and their period is closer to zero with rising D and decreasing ϕ_c (in range from 0° to 90°). Finding a relation for the position of the peaks is more complex for $M > 2$.

Analysis of (25) for incoherent noise ($\bar{\Gamma}_{uu} = 0$) shows that the $NR = M$.

A theoretical shape of the NR_{DAS} for diffuse noise in Fig. 11 is obtained by inserting the average coherence of the diffuse noise 8 in 25. The graphs show that the NR_{DAS} is greater for greater number of microphones. The NR is increasing with increasing frequency in the case of diffuse noise. Diffuse noise is omnidirectional and the directivity of DAS increases with increasing frequency.

A comparison of the theoretical shapes and simulations

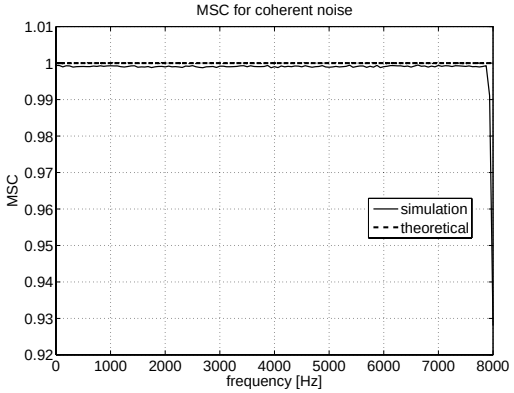

Fig. 8. Comparison of MSC for model and simulation and coherent noise, D = 5 cm.

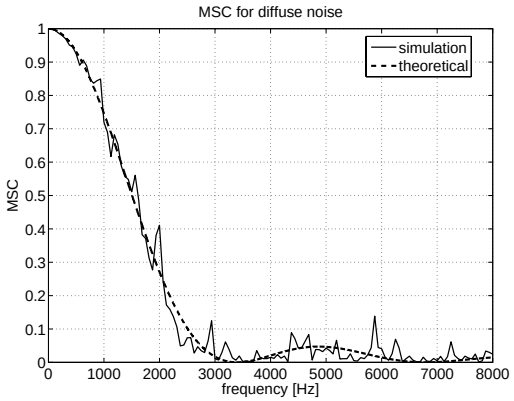

Fig. 9. Comparison of MSC for model and simulation and diffuse noise, D = 5 cm.

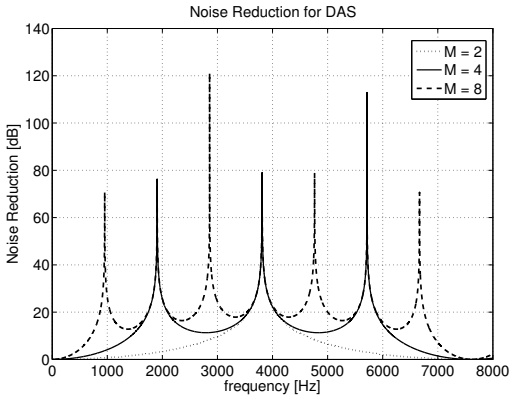

Fig. 10. Theoretical NR for coherent noise and DAS. M = $2, 4, 8$.

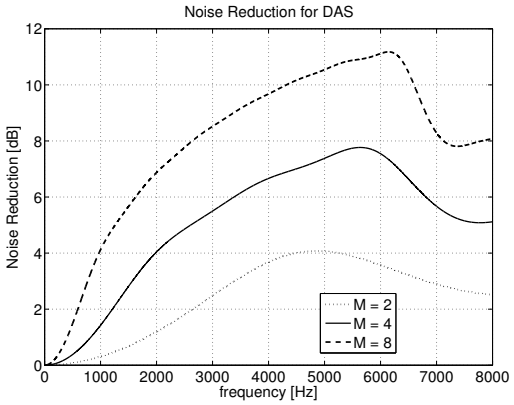

Fig. 11. Theoretical NR for diffuse noise and DAS. M = $2, 4, 8$.

is depicted in Figs. 12 and 13 for coherent and diffuse noise, respectively. The graphs show that the simulations follow the theoretical behavior.

6.4 BAP

The results of analyses and simulations for BAP are depicted in Figs. 14 – 17. The shapes of analyses for coherent noise (Fig. 14) and for diffuse noise (Fig. 15) were also obtained by inserting the average coherence in (30) for NR_{BAP}. Figure 14 shows that BAP does not almost perform reduction of coherent noise. The peaks which are caused by the zero values of the denominator of the NR are viewed in the figure. The location of the peaks is similar to DAS.

BAP shows a better performance for diffuse noise. The analyses are depicted in Fig. 15. The peaks correspond to the zero values of the denominator of the NR_{BAP}.

BAP reaches the best performance for incoherent noise. Let us insert the coherence of incoherent noise $\Gamma_{uu}(e^{j\omega T}) = 0$ in NR_{BAP} 30. The denominator is equal to zero, and NR_{BAP} reaches almost infinite values in the whole frequency range.

Real performance of BAP differs from the analyses, see Fig. 16 and Fig. 17. The peaks of the NR are smoothed in simulations.

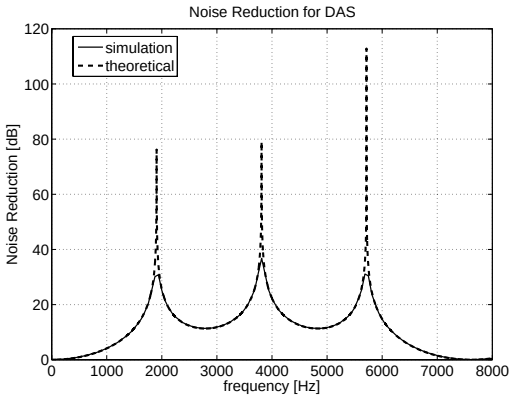

Fig. 12. Comparison of theoretical NR and simulation for coherent noise and DAS. M = 4.

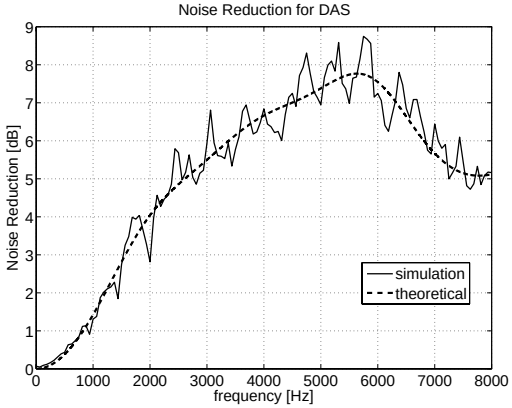

Fig. 13. Comparison of theoretical NR and simulation for diffuse noise and DAS. M = 4.

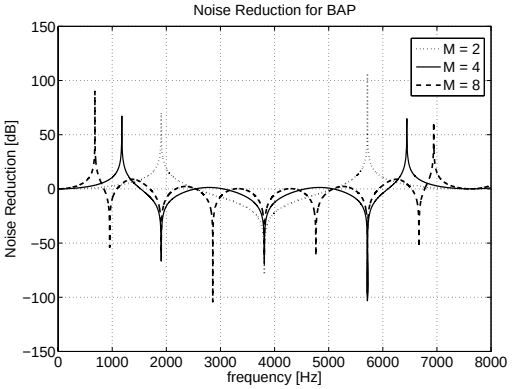

Fig. 14. Theoretical NR for coherent noise and BAP. M = 2, 4, 8.

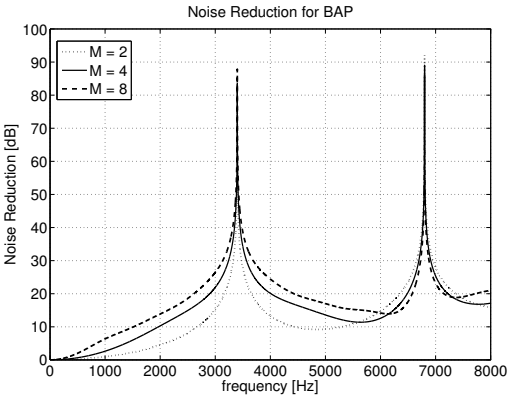

Fig. 15. Theoretical NR for diffuse noise and BAP. M = 2, 4, 8.

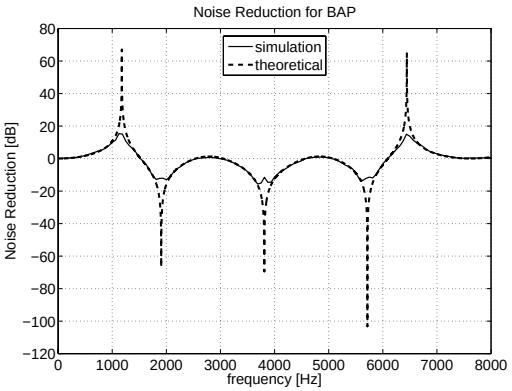

Fig. 16. Comparison of theoretical NR and simulation for coherent noise and BAP. M = 4.

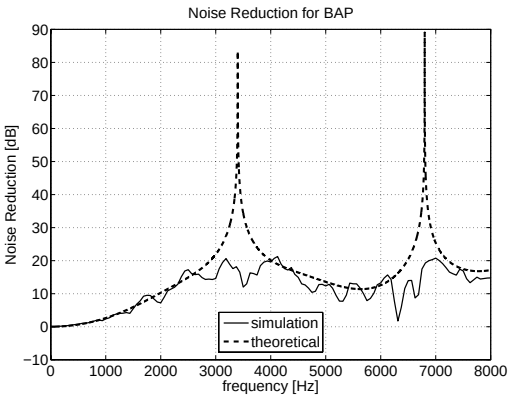

Fig. 17. Comparison of theoretical NR and simulation for diffuse noise and BAP. M = 4.

6.5 GSC

The results of analyses and simulation of GSC are depicted in Figs. 18 – 21. GSC performs almost complete suppression of coherent interference without reference to number of channels (see Fig. 18). The ability of GSC to suppress coherent noise is given by the ANC filter. ANC suppresses coherent noise independently on frequency. The shapes of the *NR* are almost identical for various number of channels.

The results of the simulations of GSC and coherent noise (Fig. 20) demonstrate high sensitivity of the NR_{GSC} to fulfill the model assumptions. The modeled input signal does not fulfill the condition (7) that means it is impossible to generate fully coherent noise. A mild deviation from the assumptions (Fig. 8) results in the decrease of the *NR* by almost 120 dB. Despite this decrease, the *NR* is about 40 dB.

The performance of GSC is the same as DAS in the case of incoherent noise. Let us insert the average coherence of incoherent noise $\bar{\Gamma}(e^{j\omega T}) = 0$ in (35). The second term of the denominator of this relation is equal to zero. The properties of $|\mathfrak{U}|^2$ are obvious after inserting of $\Gamma^u_{X_iX_k} = 0$ in (31). This insertion results in $|\mathfrak{U}|^2 = 0$. The denominator of (35) contains only the term $\heartsuit$, which is the denominator of NR_{DAS}. The NR_{GSC} is equal to M in case of incoherent noise.

GSC cannot suppress diffuse noise. Theoretical shapes of the NR_{GSC} are close to the shapes of the NR_{DAS}. Both of these shapes can be compared in Section 6.9, Fig. 34. The performance of GSC in simulation is almost identical to the analysis in case of diffuse noise (Fig. 21).

6.6 LCB

The shapes of analyses and simulations of LCB are depicted in Figs. 22 – 25. The NR_{LCB} is given by (38). LCB combines the properties of BAP and GSC. The analysis of LCB for coherent noise (Fig. 22) shows the high values of the *NR*. This performance is similar to that of GSC. The negative peaks of the NR_{LCB} occur at the same positions as the peaks of NR_{DAS}.

The performance of LCB (Fig. 25) is close to the performance of BAP (17) in the case of diffuse noise.

In the case of incoherent interference ($\bar{\Gamma}_{uu}(e^{j\omega T}) = 0$), (38) for NR_{LCB} is transformed to (30) for NR_{BAP}. After inserting of $|\mathfrak{U}|^2 = 0$ in (38), formula $NR_{LCB} = \frac{\heartsuit}{\bar{\Gamma}_{uu^2}}$ is obtained. This final formula represents the NR_{BAP}. LCB performs the complete rejection of incoherent noise as well as BAP does.

The result of the simulation of LCB (Fig. 24) demonstrates a high sensitivity of the performance of LCB to keep model assumptions. The result of the simulation shows that LCB almost does not perform noise reduction.

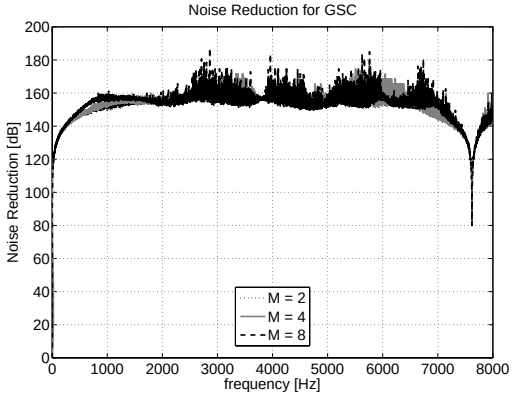

Fig. 18. Theoretical *NR* for coherent noise and GSC. M = 2,4,6,8.

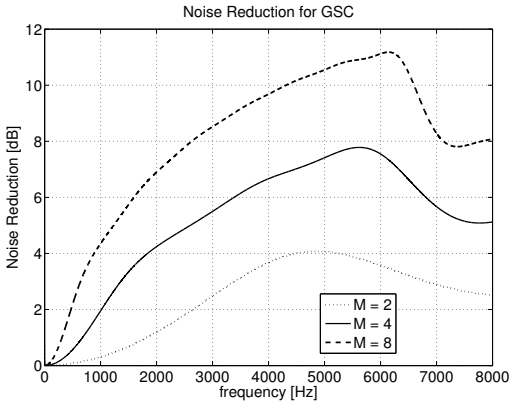

Fig. 19. Theoretical *NR* for diffuse noise and GSC. M = 2,4,6,8.

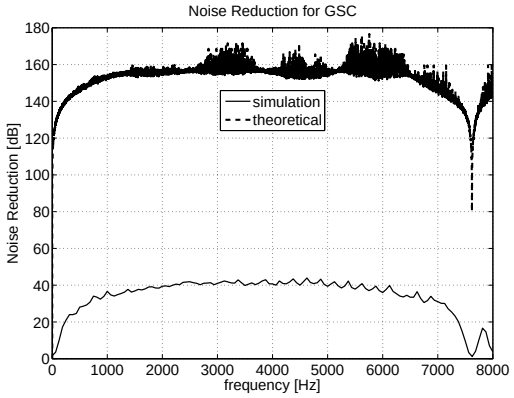

Fig. 20. Comparison of theoretical *NR* and simulation for coherent noise and GSC. M = 4.

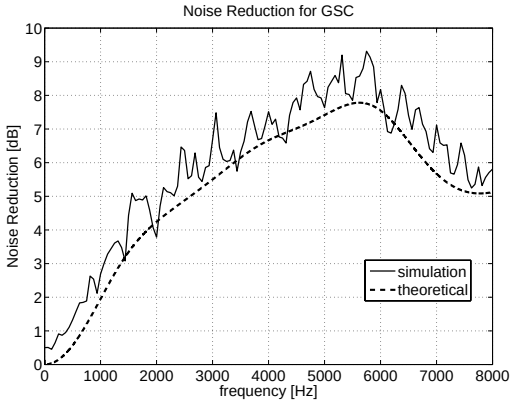

Fig. 21. Comparison of theoretical *NR* and simulation for diffuse noise and GSC. M = 4.

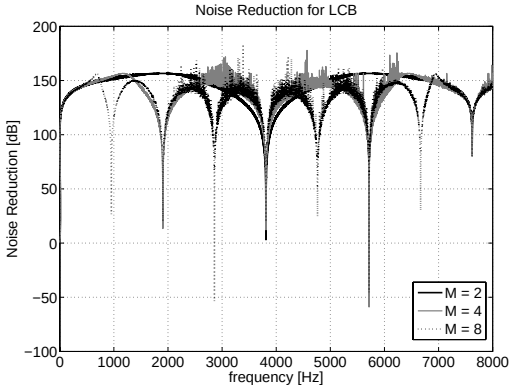

Fig. 22. Theoretical *NR* for coherent noise and LCB. M = 2, 4, 8.

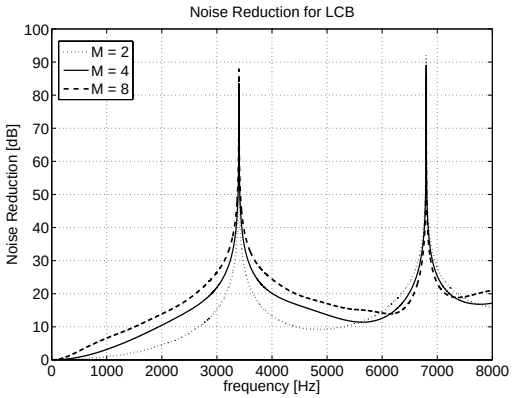

Fig. 23. Theoretical *NR* for diffuse noise and LCB. M = 2, 4, 8.

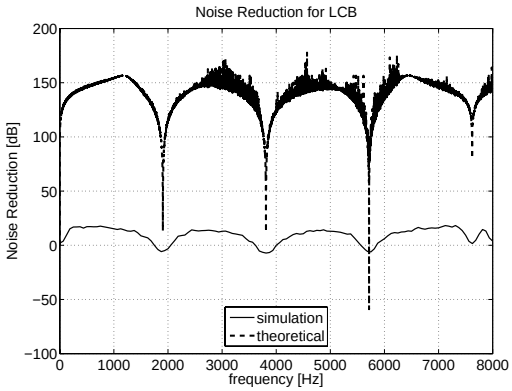

Fig. 24. Comparison of theoretical *NR* and simulation for coherent noise and LCB. M = 4.

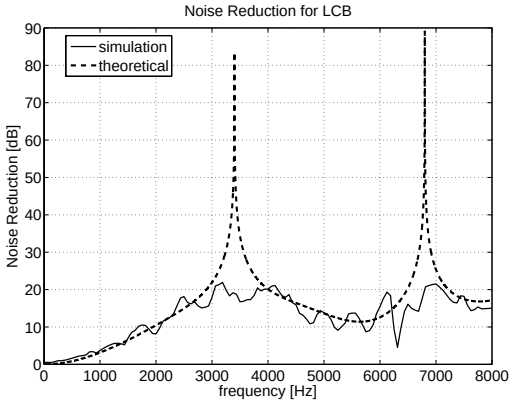

Fig. 25. Comparison of theoretical *NR* and simulation for diffuse noise and LCB. M = 4.

The result of the simulation of LCB for diffuse noise (Fig. 25) is very close to the result of the analysis.

6.7 MCF

The Figs. 26 – 28 and Fig. 10 show the performance of MCF. The shapes in the figures represent the situation when $|\Gamma_{ij}|^2 \leq \mathrm{T}$. Otherwise, the shapes would be the same as the shapes for BAP. The theoretical shape of the NR_{MCF} is obtained by inserting the coherence in (39).

In the case of coherent interference ($|\Gamma_{ij}|^2(e^{\mathrm{j}\omega T}) = 1$), the performance of MCF is the same as DAS. The shape of NR_{MCF} for coherent interference is depicted in Fig. 10.

The performance of MCF is the same as DAS also in the case of incoherent noise. Inserting $|\Gamma_{ij}|^2(e^{\mathrm{j}\omega T}) = 0$ in (39) results in $NR_{MCF} = \mathrm{M}$.

MCF reaches the highest *NR* in comparison with all other systems in the case of diffuse noise.

The simulation of MCF (Fig. 27) for coherent noise showed the same result as the simulation of DAS. The result of simulation for diffuse noise differs from the analysis (Fig. 28). The result of the simulation of MCF is the best among all other systems.

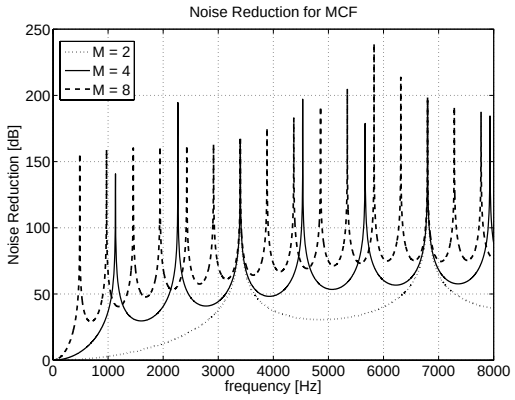

Fig. 26. Theoretical *NR* for diffuse noise and MCF according to Eq. (40). M = 2, 4, 8.

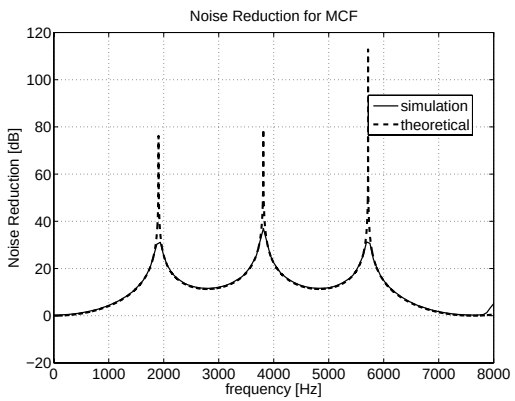

Fig. 27. Comparison of theoretical *NR* and simulation for coherent noise and MCF. M = 4.

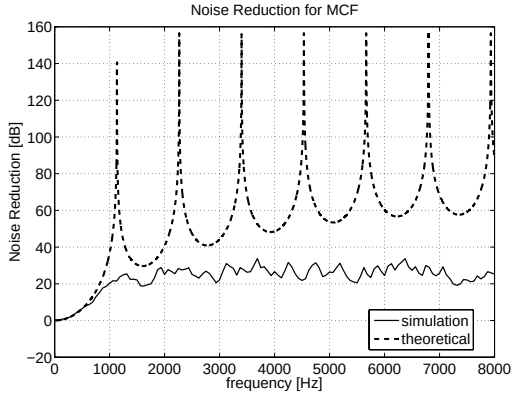

Fig. 28. Comparison of theoretical *NR* and simulation for diffuse noise and MCF. M = 4.

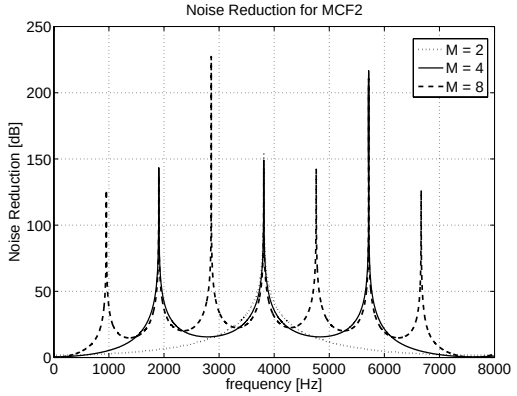

Fig. 29. Theoretical *NR* for coherent noise and MCF2 according to Eq. (43). M = 2, 4, 8.

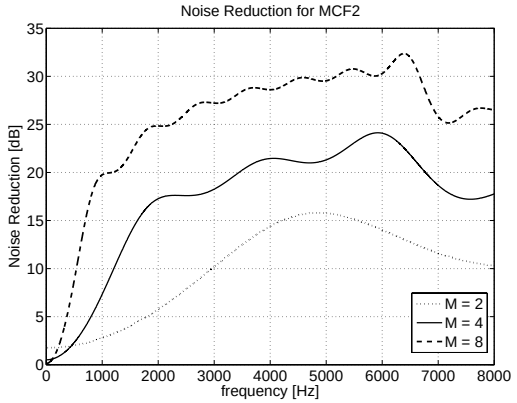

Fig. 30. Theoretical *NR* for diffuse noise and MCF2 according to Eq. (43). M = 2, 4, 8.

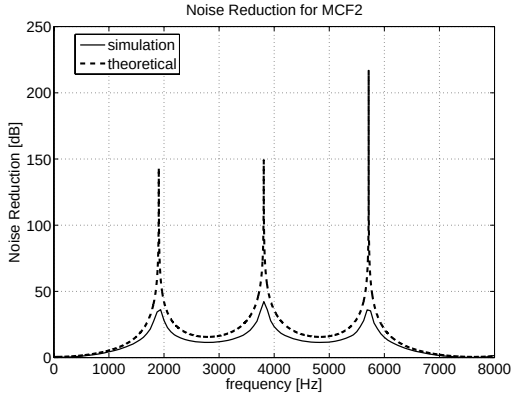

Fig. 31. Comparison of theoretical *NR* and simulation for coherent noise and MCF2. M = 4.

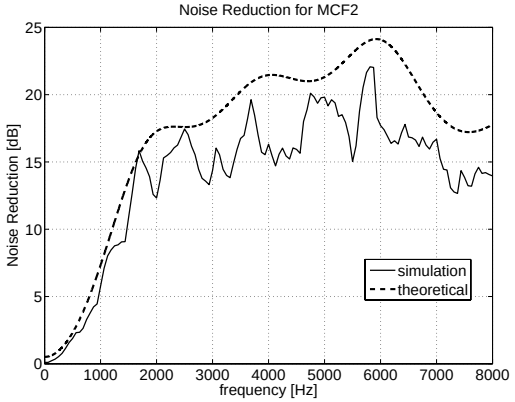

Fig. 32. Comparison of theoretical *NR* and simulation for diffuse noise and MCF2. M = 4.

6.8 MCF2

The shapes of the analyses and simulation of MCF2 are depicted in Figs. 29 – 32. The theoreticall shape of the NR_{MCF2} was obtained by inserting of the coherence in (43) (Fig. 29). This shape is very similar to the shape of the NR_DAS (Fig. 10). The positions of the peaks are also given by the zero points of the denominator of the NR_{MCF2}.

The analyses of MCF2 for diffuse noise are depicted in Fig. 30. The performance is also similar to the performance of DAS.

The idea about the performance of MCF2 in the case of incoherent noise can be obtained by analysis of (43). Inserting $\Gamma_{uu} = 0$ promises a complete reduction of incoherent interference.

The results of the simulations (Figs. 27 and 32) are very similar to the shapes of the analyses.

6.9 Comparison of All Systems

The results of the analyses and simulations showed the ability of the systems to reduce the interference. A comparison of the analyses of all systems is depicted in Fig. 33 and Fig. 34 for coherent and diffuse noise, respectively. The highest values of the *NR* were reached by GSC and LCB. However, the simulations revealed high sensitivity of these systems to violation the assumptions about the input signals.

The highest reduction of diffuse noise was reached by MCF and MCF2. This fact was verified by the simulations (Figs. 28, 32). The graph in Fig. 34 reveals a very similar performance of DAS and GSC and also very similar performance of BAP and LCB for diffuse noise.

7. Conclusion

The *NR* for five kinds of the noise reducing systems were theoretically evaluated with the aim to compare their efficiency in noise suppression. The *NR* was expressed in

dependence on coherence so that the influence of noise type can be discussed. Due to the dependence of the *NR* on coherence, the influence of type of noise could be then discussed. The *NR* shows only the influence of the system on interference. The *NR* does not respect the influence of the system on the desired signal. In this case, this criterion should be combined with other suitable criteria [12].

The theoretical derivation of the *NR* is crucial for the analyses of beamformers and for the design of their modification. The formulas derived in this paper will be utilized in further work for development of advanced methods of noise suppression.

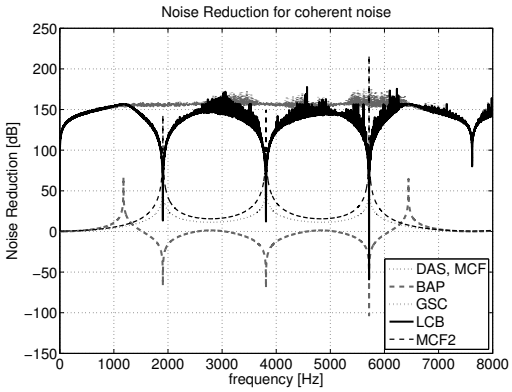

Fig. 33. Comparison of the theoretical NR for coherent noise.

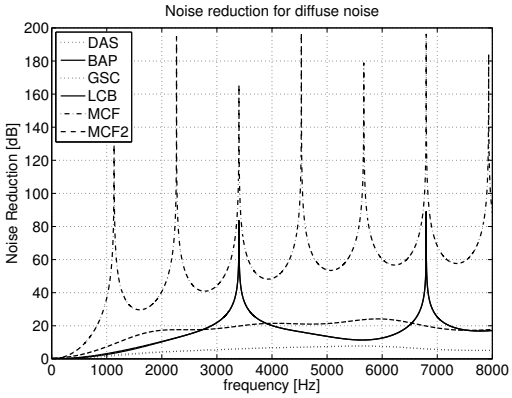

Fig. 34. Comparison of the theoretical NR for diffuse noise.

Acknowledgements

This paper was mainly supported by research activity MSM 6840770012 "Transdisciplinary Research in Biomedical Engineering II" and GACR grant GD102/08/H008 "Analysis and modeling of biomedical and speech signals" and GACR grant GA102/08/0707 "Speech Recognition under Real-World Conditions".

References

[1] BITZER, J., SIMMER, K. U., KAMMEYER, K.-D. Theoretical noise reduction limits of the generalized sidelobe canceller (GSC) for speech enhancement. In *International Conference on Acoustics, Speech, and Signal Processing ICASSP '99. Vol. 5*. Phoenix (USA), 1999. p. 2965–2968.

[2] BOUQUIN, R. L. Enhancement of noisy speech signals: application to mobile radio communications. *Speech Communication*, 1996, vol. 18, no. 1, p. 3–19.

[3] CRON, B. F., SHERMAN, C. H. Spatial-correlation functions for various noise models. *Journal of Acoustic Society of America*, 1962, vol. 34, no. 11.

[4] FISCHER, S., SIMMER, K. U. Beamforming microphone arrays for speech acquisition in noisy environments. *Speech Communication*, 1996, vol. 20, p. 215–227.

[5] FROST, O. L. An algorithm for linearly constrained adaptive array processing. In *IEEE*, 1972, vol. 60, p. 926–934.

[6] GRIFFITHS, L. J., CHARLES, W. J. An alternative approach to linearly constrained adaptive beamforming. *IEEE Transaction on Antenas and Propagation*,1982, vol. AP-30, no. 1.

[7] INGERLE, J. *Methods of Speech Signal Enhancement Combining Beamforming and Postfiltration*. PhD thesis, Prague: FEL, Czech Technical University, 2003. In Czech.

[8] MAHMOUDI, D., DRYGAJLO, A. Combined Wiener and coherence filtering in wavelet domain for microphone array speech enhancement. In *Proceedings of the 1998 International Conference on Acoustics, Speech and Signal Processing. Vol. 1.* Seattle (USA), 1998, vol. 1, p. 385–388.

[9] MARRO, C., MAHIEUX, Y., SIMMER, K. U. Analysis of noise reduction and dereverberation techniques based on microphone arrays with postfiltering. *IEEE Transactions on Speech and Audio Processing*, 1998, vol. 6, no. 3, p. 240–259.

[10] MEYER, J., SIMMER, K. U. Multi-channel speech enhancement in a car environment using Wiener filtering and spectral subtraction. In*International Conference on Acoustics, Speech, and Signal Processing ICASSP '97. Vol. 2*. Munich (Germany), 1997, p. 1167–1170.

[11] RAFAELY, B. Spatial-temporal correlation of a diffuse sound field. *The Journal of the Acoustical Society of America*, 2000, vol. 107, no. 6, p. 3254–3258.

[12] SIMMER, K. U., BITZER, J., MARRO, C. Post-filtering techniques *Microphone Arrays*. Berlin: Springer, 2001, p. 39–57.

[13] SIMMER, K. U., WASILJEFF, A. Adaptive microphone arrays for noise suppression in the frequency domain. In *COST-229 Workshop on Adaptive Algorithms in Communications.* Bordeaux (France), 1992, p. 185–194.

[14] SOVKA, P., POLLÁK, P. *Chosen Methods of Digital Signal Processing*. Prague: CTU Publishing House, 2003. In Czech.

[15] UHLÍŘ, J., SOVKA, P. *Digital Signal Processing*. Prague: CTU Publishing House, 2002. In Czech.

[16] VAN VEEN, B. D., BUCKLEY, K. M. Beamforming: A versatile approach to spatial filtering. *IEEE ASSP Magazine*, 1988, p. 4–24.

[17] ŠTRUPL, M., SOVKA, P. Analysis and simulation of frost's beamformer. *Radioengineering*, 2003, vol. 12, no. 3, pp. 1–9.

[18] WIDROW, B., STEARNS, S. D. *Adaptive Signal Processing*. Prentice-Hall, 1985.

[19] ZELINSKI, R. A microphone array with adaptive post-filtering for noise reduction in reverberant rooms. In *International Conference of Acoustic Speech Signal Processing.* New York (USA), 1988, p. 2578–2581.

About Authors...

Václav BOLOM was born in 1980 in Prague, Czech Republic. He received the M.S. degree in electrical engineering from FEE CTU in Prague in 2006. He is a Ph.D. student at the Department of Circuit Theory at FEE CTU in Prague. His research interest includes multichannel and adaptive signal processing.

Jan INGERLE was born in 1976 in Nové Město na Moravě, Czech Republic. He received the M.S. degree in electrical engineering from FEE CTU in Prague in 2000, and Ph.D. degree from the Department of Cuircuit Theory, FEE CTU in Prague in 2004. Until 2008, he worked at ST Microelectronics in Prague as a digital radio algorithm developer. Currently, he works as a software developer at Voice Technologies and Systems Research and Development Lab, Whatson Research at IBM in Prague. His research interests include speech and audio processing and speech recognition algorithms.

Pavel SOVKA was born in Jihlava, Czech Republic, in 1957. He received the M.S. and Ph.D. degrees in electrical engineering from the Faculty of Electrical Engineering, Czech Technical University Prague (FEE CTU) in 1981 and 1986, respectively. From 1985 to 1991 he worked in the Institute of Radioengineering and Electronics of the Czech Academy of Sciences, Prague. In 1991, he joined the Department of Circuit Theory, FEE CTU. Since 1996, he has been an associate professor. Among his current research interests is the application of adaptive systems to noise and echo cancellation, speech analysis, chengepoint detection, signal separation. Mr. Sovka is a member of the European Speech Communication Association (ESCA).